NACA RM L52C27

NACA

RESEARCH MEMORANDUM

AN APPLICATION OF THE ROCKET-PROPELLED-MODEL TECHNIQUE TO THE INVESTIGATION OF LOW-LIFT BUFFETING AND THE RESULTS OF PRELIMINARY TESTS

By Homer P. Mason and William N. Gardner

Langley Aeronautical Laboratory
Langley Field, Va.

NATIONAL ADVISORY COMMITTEE
FOR AERONAUTICS

WASHINGTON
September 2, 1952
Declassified November 2, 1954

NATIONAL ADVISORY COMMITTEE FOR AERONAUTICS

RESEARCH MEMORANDUM

AN APPLICATION OF THE ROCKET-PROPELLED-MODEL TECHNIQUE TO THE INVESTIGATION OF LOW-LIFT BUFFETING AND THE RESULTS OF PRELIMINARY TESTS

By Homer P. Mason and William N. Gardner

SUMMARY

The rocket-propelled-model technique has been applied to the investigation of low-lift buffeting. Results of preliminary tests show that severe buffeting, wing dropping, and normal-force changes occur almost simultaneously near zero lift over a Mach number range near 0.9 on unswept wings 12 percent thick. On unswept wings 7 percent thick, buffeting did not occur; however, mild wing dropping and normal-force changes were experienced.

INTRODUCTION

The low-lift high-speed buffet characteristics of modern aircraft have been of major importance for some time. Flight tests have been conducted to define these characteristics in the form of buffet boundaries. These boundaries usually are presented in terms of the lift coefficient, as a function of Mach number, at which the pilot or an accelerometer first senses the buffet oscillation. Some tests and buffet boundaries thus determined are described in references 1 to 3.

A study of available buffet data indicates that in most cases the boundaries may be extended to zero lift at high subsonic Mach numbers. A simple zero-lift rocket-propelled research model has been developed to study the mechanics of this phenomenon as it is affected by such factors as wing section, sweepback, and tail junctures. The purpose of this paper is to illustrate the application of this technique to the investigation of low-lift buffeting and to present the data obtained from flight tests of three models.

SYMBOLS

c	wing chord
R	Reynolds number, based on mean aerodynamic chord
M	free-stream Mach number
p	rolling velocity, radians per second
V	free-stream velocity, feet per second
b	wing span, feet
pb/2V	trim wing-tip helix angle, radians
q	free-stream dynamic pressure, pounds per square foot
S	wing area (total in one plane), square feet
N	normal force, pounds
$C_{N_{trim}}$	trim normal-force coefficient (N/qS)
D	drag, pounds
C_D	total drag coefficient (D/qS)
p_s	local static pressure, pounds per square foot
p_o	free-stream static pressure, pounds per square foot
P	pressure coefficient $\left(\frac{p_s - p_o}{q}\right)$

Subscripts:

2,3	indicate orifice at which pressure coefficient was determined

TECHNIQUE AND TESTS

Analysis of previous buffet research data (refs. 1 to 4) leads to the conclusion that high-speed low-lift buffeting is a result of

shock-induced flow separation. Since this type of flow separation may occur near zero lift (refs. 2 and 5) and is primarily a function of thickness ratio and surface contour, buffeting may occur at zero lift on either a wing, tail, or body, or at the juncture of two aerodynamic surfaces. Thus, the presence of an aerodynamic surface in a disturbed wake is not essential for this type of buffeting. The rocket-propelled-model technique offers a relatively simple method for the investigation of this type of buffeting through measurements of normal accelerations and vibration frequencies in free flight of simple research vehicles utilizing wings having various geometric characteristics.

Test Vehicle

A parabolic body of revolution having a fineness ratio of 10, maximum diameter at the 50-percent body station, and base diameter 0.384 maximum diameter was chosen because of its near optimum drag characteristics and aerodynamic cleanness (ref. 6). A special nozzle, designed to provide an essentially straight jet, was installed to minimize any induced flow disturbances due to the sustainer rocket motor. Test wings having aspect ratio 4, taper ratio 0.5, NACA 65A airfoil sections, and zero sweep at the 60-percent chord were mounted in a cruciform tail arrangement with the intersection of the 25-percent chord line and the body centerline at the 80-percent body station. At this body station the wing span was approximately 5.3 body diameters. General specifications of the test configuration are shown in figure 1.

Instrumentation

Two accelerometers were located in the body at the 25-percent chord of the test wings and another was located in the nose section at the 37.5-percent body station to measure the buffet frequencies and magnitudes normal to one of two sets of 7-percent-thick wings on one model and normal to the 12-percent-thick wings of another model having both 7- and 12-percent-thick wings. Absolute body pressures were measured on a plane midway between the wings at the 50.5-, 83.3-, 90.5-, and 96-percent body stations on a third model which had 6-percent-thick wings. Longitudinal accelerometers were used to measure the drag of the complete configurations. Accelerometer and pressure measurements were transmitted to the ground station during flight by means of the NACA telemetering system. Velocity and flight-path data were obtained from Doppler and tracking radar. Roll data were obtained from spinsonde recorders and atmospheric data were obtained from radiosondes released after each flight.

Tests

Three models were tested to determine whether this technique is adequate for measuring or sensing buffeting, whether any buffeting experienced could be attributed to a single variable (in this case, wing thickness), and whether there were any induced flow disturbances due to the sustainer-rocket-motor jet. One model incorporated an NACA 65A007 (approx.) airfoil section parallel to free stream on all four wings. The second model had NACA 65_1A012 airfoil sections on the wings in one plane and 65A007 (approx.) airfoil sections on the wings in the other plane. The third model had NACA 65A006 airfoil sections on all four wings. All wings were of wood-core construction with surface inlays and trailing-edge inserts of aluminum alloy.

Flutter speeds were estimated for all wings and found to be well above the maximum flight speeds. The first-bending natural frequency of all wings was measured prior to flight tests and found to be of the order of 100 to 110 cycles per second. The natural frequency of a typical accelerometer used was approximately 75 cycles per second. It has been shown that accelerometers of the type used are capable of following wing oscillations of 250 cycles per second or higher, although the amplitude response is reduced at frequencies much above the instrument natural frequency. Models were accelerated to a Mach number of approximately 0.8 by a 5-inch high-performance booster and, after booster separation, the models were accelerated slowly (approximately 0.15 Mach number per second) to a maximum Mach number of approximately 1.4 by a built-in sustainer rocket motor. Data were obtained continuously throughout the entire flight of each model. Photographs of the general model configuration and one model-booster combination are shown in figures 2 and 3, respectively. Test Reynolds numbers based on the wing mean aerodynamic chord of 0.619 foot are shown in figure 4 as a function of Mach number.

Flight tests were conducted at the Langley Pilotless Aircraft Research Station at Wallops Island, Va.

RESULTS AND DISCUSSION

Buffeting

A reproduction of the actual accelerometer records obtained from the flight of the model having 12-percent-thick wings is shown in figure 5 for the complete range of low-lift buffeting. Low-lift buffeting occurred between Mach numbers of 0.85 and 0.97 during accelerating flight and 0.97 and 0.88 during decelerating flight. These Mach numbers define

the points at which a definite increase in the intensity of the oscillating accelerometer trace can be detected and may or may not define the actual boundary for initial buffeting. No explanation is available for the fact that the low Mach number boundaries are not coincident during accelerating and decelerating flight. The recorded buffet frequency was approximately 120 cycles per second which is of the same order as the wing first-bending natural frequency. The maximum amplitude of the buffet oscillation was approximately ±2.5g which corresponds to a variation of normal-force coefficient of approximately ±0.10. This amplitude would be considered severe since the wing loading of the test vehicle was of the order of 50 pounds per square foot. Even though the recorded buffet oscillations are irregular in both frequency and amplitude (fig. 5), there is a gradual build-up to a maximum intensity followed by a gradual decrease of intensity as the buffet Mach number region is traversed.

Accelerometer records obtained from the flight of the model having 7-percent-thick wings were consistently smooth throughout the entire speed range of the test and gave no indication of the occurrence of buffeting. The model having 6-percent-thick wings had no normal accelerometer; hence, no direct buffet data are available. Pressure measurements on this model indicated no jet-induced flow disturbances.

In comparing these buffet data with those presented in reference 1, it is noted that the Mach number at which buffeting occurred on the 12-percent-thick wing agrees with previous experience; however, no buffeting was indicated for the 7-percent-thick wing which is above the airfoil thickness ratio - Mach number boundary shown in reference 1. In this reference, however, it should be noted that the thinnest smooth-contoured wing on which buffeting was encountered was 8 percent thick; hence, the absence of buffeting on the 7-percent-thick wing in the present test must be considered as additional, rather than contradictory, data, since no test data on 7-percent-thick wings were shown in reference 1.

On the basis of the data obtained from the present tests and their correlation with previously determined data, it may be concluded that the rocket-propelled-model technique is adequate for the qualitative investigation of buffet phenomenon.

Wing Dropping

The trim wing-tip helix angles $pb/2V$ for all models are plotted against Mach number in figure 6. These data show severe wing dropping of the 12-percent-thick wing and mild wing dropping of the 6- and 7-percent-thick wings. Wing dropping on the 12-percent-thick wing

occurred at a Mach number of 0.88 which is above the wing-dropping airfoil-thickness-ratio boundary presented in reference 1. For the 6- and 7-percent-thick wings, wing dropping occurred at a Mach number of 0.89 which is below the reference boundary. These data lend emphasis to the idea advanced in reference 1 that wing thickness and contour apparently are not the only factors influencing wing dropping. Wing dropping was not experienced on the unswept 6-percent-thick smooth-contour wings of references 1 and 7. The wings of references 1 and 7 were mounted on a cylindrical body, whereas in the present tests, the wings were mounted on a parabolic body. This fact may indicate that interference effects are an influencing factor in causing wing dropping. Although it is felt by some authors that wing dropping may be induced by a change in effective dihedral with Mach number (ref. 8), it is believed that any such effects are negligible for the symmetrical configurations of the present tests.

Figure 7 is a plot of the variation of pressure coefficient with Mach number as determined from the four body pressure orifices on the 6-percent-thick-wing model. These data show large and rapid pressure changes at the two orifices located nearest the wings, particularly over the Mach number range where wing dropping was experienced. As noted in figure 7, orifice number 3 is located at the 83.3-percent body station which is slightly behind the wing maximum thickness, and orifice number 2 is located at the 90.5-percent body station which is slightly behind the wing trailing edge. Figure 8 is a plot against Mach number of the variation of the pressure-coefficient gradient between orifice number 3 and orifice number 2. The data show a very rapid change in gradient from a high positive value to a high negative value over the Mach number range where wing dropping was experienced. This rapid change in pressure gradient would seem to accentuate unsymmetrical flow conditions resulting in marked changes in unsymmetrical lift loads on opposite panels and a rolling moment and would thus contribute to the wing-dropping phenomenon.

The Mach numbers at which the low-lift buffet-intensity rise occurred on the 12-percent-thick wing are also shown in figure 6. A close relationship between wing dropping and buffeting is immediately apparent, in that the Mach number range over which wing dropping occurs is practically the same as the buffet Mach number range. No explanation can be given at this time for the fact that buffeting did not occur on the 7-percent-thick wings over the Mach number range where wing dropping occurred; however, the wing dropping on this model was comparatively mild and this fact would indicate that a more severe flow disturbance is required to produce low-lift buffeting than is required to produce wing dropping on unswept wings having thickness ratios near 7 percent.

Trim Normal Force

The variation of trim normal-force coefficient $C_{N_{trim}}$ with Mach number is shown in figure 9 for models having 7- and 12-percent-thick wings. These trim normal-force coefficients were calculated from the mean normal acceleration determined from the 3 accelerometers in each model and are based on the total area in one plane. Again, the Mach numbers at which buffeting started and stopped on the 12-percent-thick wing are shown for comparison. As was the case for wing dropping, the change in trim normal force on the model with 12-percent-thick wings was considerably greater than on the model having 7-percent-thick wings. As would be expected, the Mach numbers at which changes in trim normal force occur correspond to the Mach numbers at which wing dropping was experienced. These tests then conclusively show that changes in trim normal force and wing dropping are two different effects of one phenomenon which is a change in lift on a wing panel. The sense of this change in lift is apparently arbitrary and unsymmetrical, but the change in lift undoubtedly is due to a shock-induced flow change behind the maximum thickness of the aerodynamic surface (ref. 9). This flow change is also responsible for low-lift buffeting; however, for essentially unswept wings with smooth contours and thickness ratios of the order of 7 percent or less, the flow disturbance is not severe enough to cause buffeting near zero lift.

Drag

Power-off drag coefficients, based on total wing area in one plane, are shown in figure 10 for all models. The model having 12-percent-thick wings also had two 7-percent-thick wings; thus, the drag difference shown is due only to the increased thickness of two of the four wing panels. The drag rise occurred at Mach numbers of approximately 0.85 for the 12-percent-thick wings and approximately 0.88 for the 6-percent-thick wings. These Mach numbers correspond to the Mach numbers at which wing dropping and the change in trim normal-force coefficient occurred.

CONCLUDING REMARKS

The rocket-propelled-model technique has been applied to the investigation of low-lift buffeting. The results of three preliminary tests utilizing this technique show that buffeting, wing dropping, and normal-force changes occur almost simultaneously near zero lift in the Mach number range from 0.85 to 0.97 on a model equipped with an unswept wing 12 percent thick. On a similar model with 7-percent-thick wings, mild wing dropping and normal-force changes occur simultaneously over a Mach

number range from 0.89 to 0.94, but the flow changes causing these phenomena are not severe enough to cause buffeting at zero lift. Wing dropping and changes in trim normal force are two different effects of a change in lift on a wing panel and may be influenced by interference effects. Buffeting at near zero lift may be expected to accompany these changes on unswept wings over 7 percent thick.

Langley Aeronautical Laboratory,
National Advisory Committee for Aeronautics,
Langley Field, Va.

REFERENCES

1. Purser, Paul E.: Notes on Low-Lift Buffeting and Wing Dropping at Mach Numbers Near 1. NACA RM L51A30, 1951.

2. Humphreys, Milton D.: Pressure Pulsations on Rigid Airfoils at Transonic Speeds. NACA RM L51I12, 1951.

3. Gadeberg, Burnett L., and Ziff, Howard L.: Flight-Determined Buffet Boundaries of Ten Airplanes and Comparisons With Five Buffeting Criteria. NACA RM A50I27, 1951.

4. Drake, Hubert M., McLaughlin, Milton D., and Goodman, Harold R.: Results Obtained During Accelerated Transonic Tests of the Bell XS-1 Airplane in Flights to a Mach Number of 0.92. NACA RM L8A05a, 1948.

5. Lindsey, W. F., Daley, Bernard N., and Humphreys, Milton D.: The Flow and Force Characteristics of Supersonic Airfoils at High Subsonic Speeds. NACA TN 1211, 1947.

6. Hart, Roger G., and Katz, Ellis R.: Flight Investigations at High-Subsonic, Transonic, and Supersonic Speeds To Determine Zero-Lift Drag of Fin-Stabilized Bodies of Revolution Having Fineness Ratios of 12.5, 8.91, and 6.04 and Varying Positions of Maximum Diameter. NACA RM L9I30, 1949.

7. Stone, David G.: Wing-Dropping Characteristics of Some Straight and Swept Wings at Transonic Speeds as Determined With Rocket-Powered Models. NACA RM L50C01, 1950.

8. Anderson, Seth B., Ernst, Edward A., and Van Dyke, Rudolph D., Jr.: Flight Measurements of the Wing-Dropping Tendency of a Straight-Wing Jet Airplane at High Subsonic Mach Numbers. NACA RM A51B28, 1951.

9. Daley, Bernard N., and Humphreys, Milton D.: Effects of Compressibility on the Flow Past Thick Airfoil Sections. NACA TN 1657, 1948.

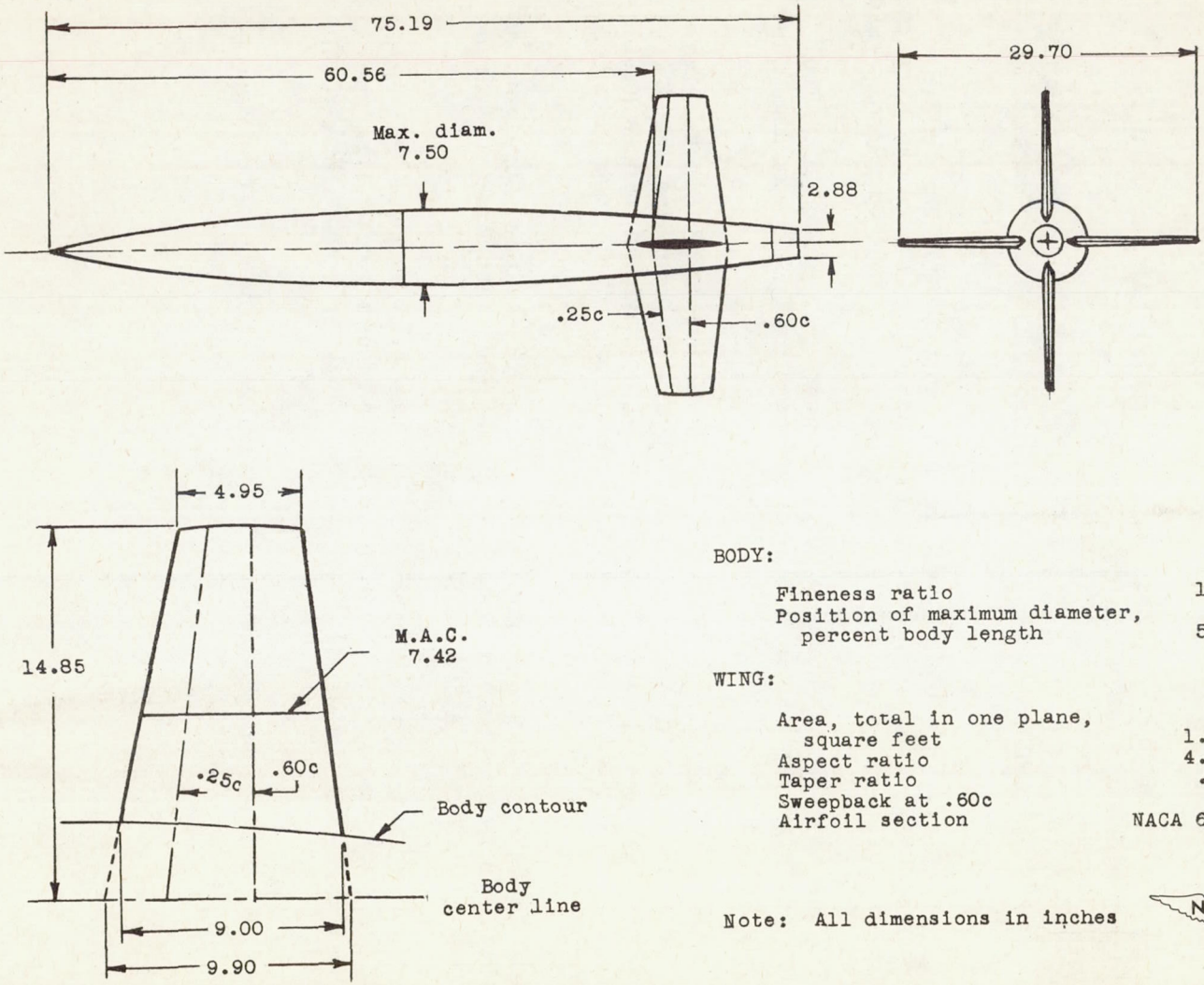

BODY:

Fineness ratio	10
Position of maximum diameter, percent body length	50

WING:

Area, total in one plane, square feet	1.53
Aspect ratio	4.00
Taper ratio	.5
Sweepback at .60c	0°
Airfoil section	NACA 65A~~6~~xx

Note: All dimensions in inches

Figure 1.- General specifications of test vehicle.

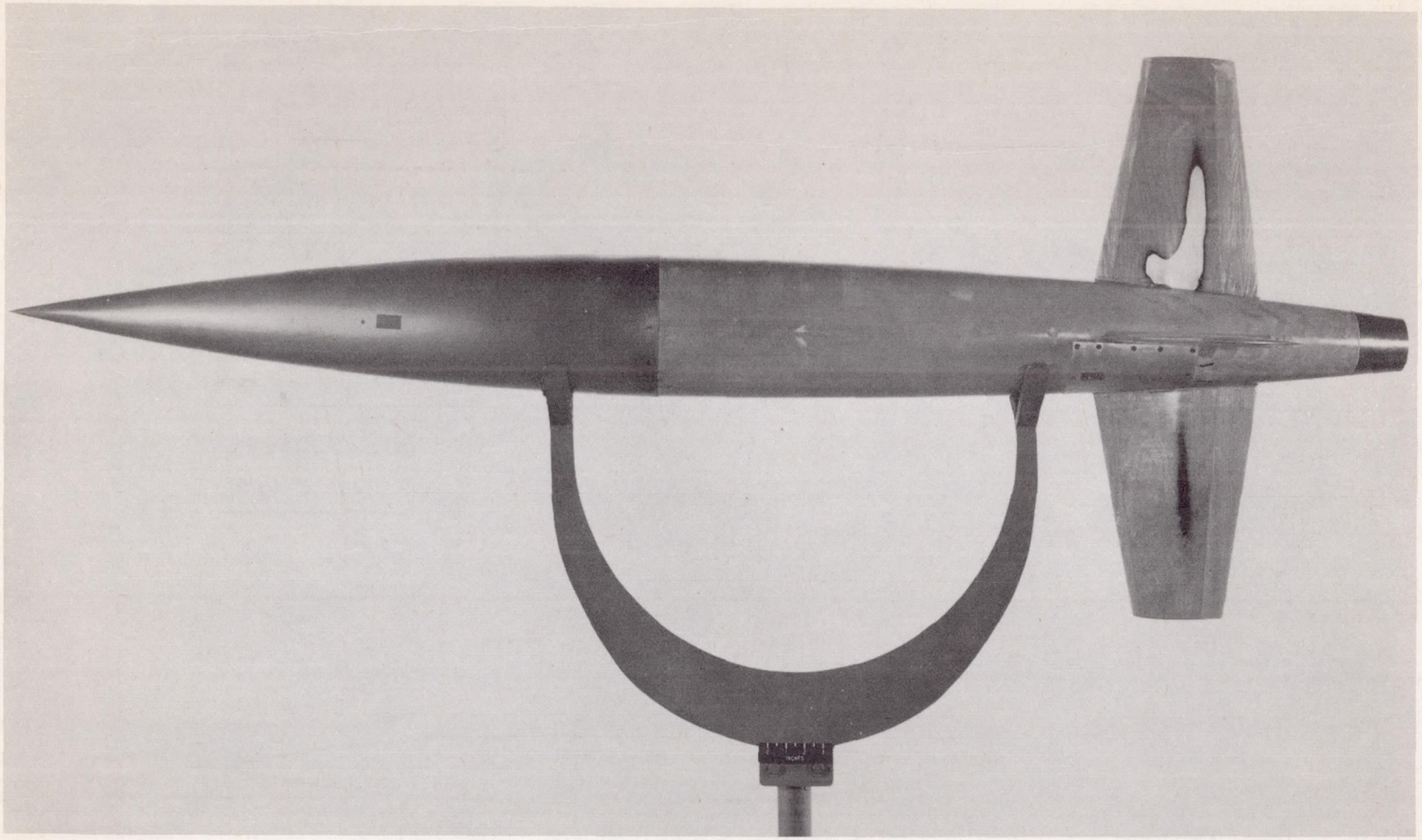

Figure 2.- General model configuration.

NACA L-67047.1

Figure 3.- Model and booster combination on launcher.

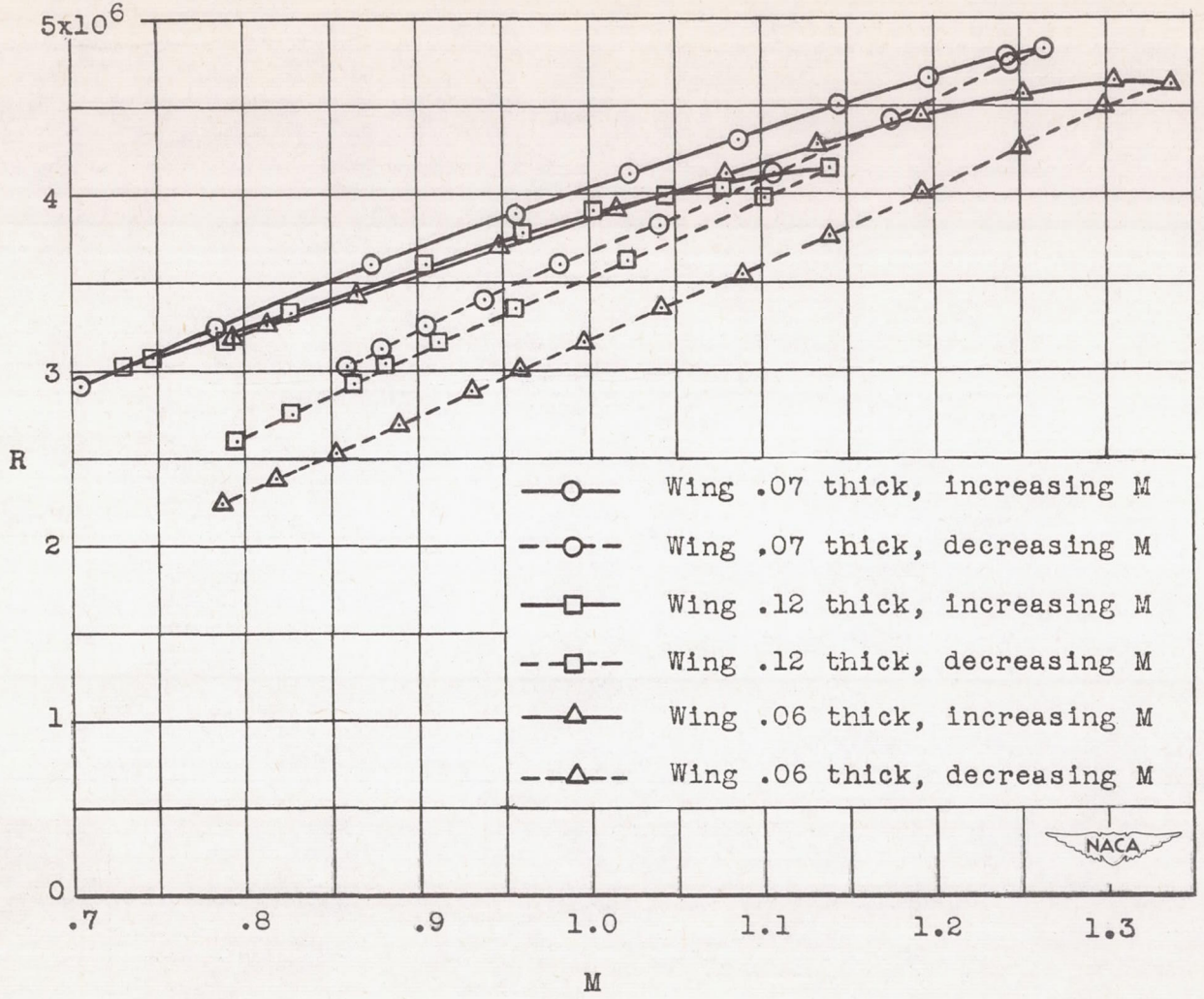

Figure 4.- Variation of Reynolds number with Mach number.

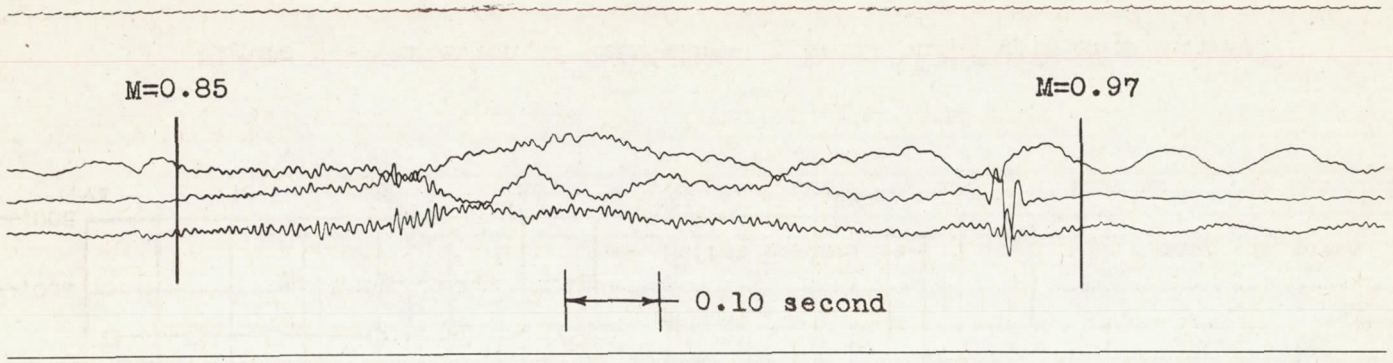

(a) Increasing Mach number.

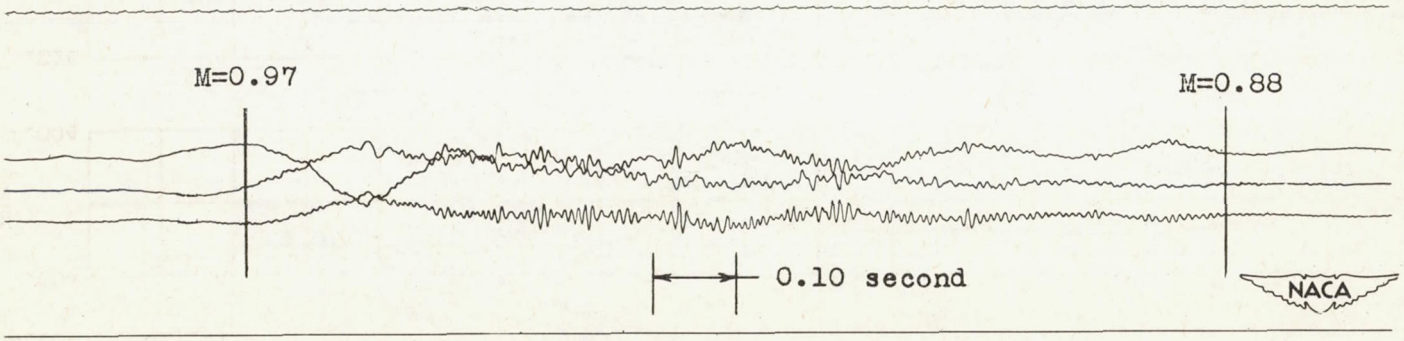

(b) Decreasing Mach number.

Figure 5.- Part of telemeter record showing normal accelerations during buffeting of model having wings 12 percent thick.

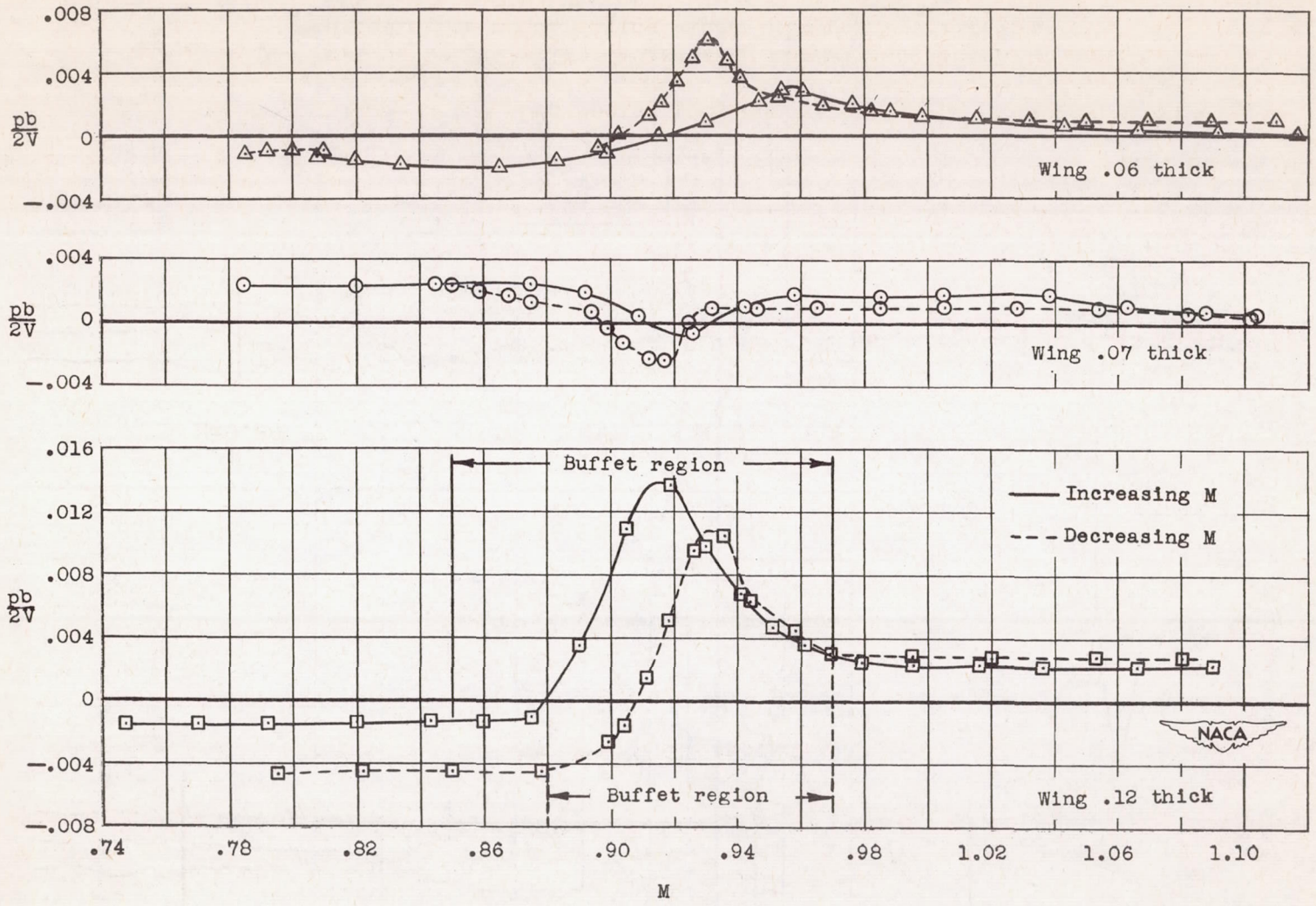

Figure 6.- Variation of trim wing-tip helix angle with Mach number.

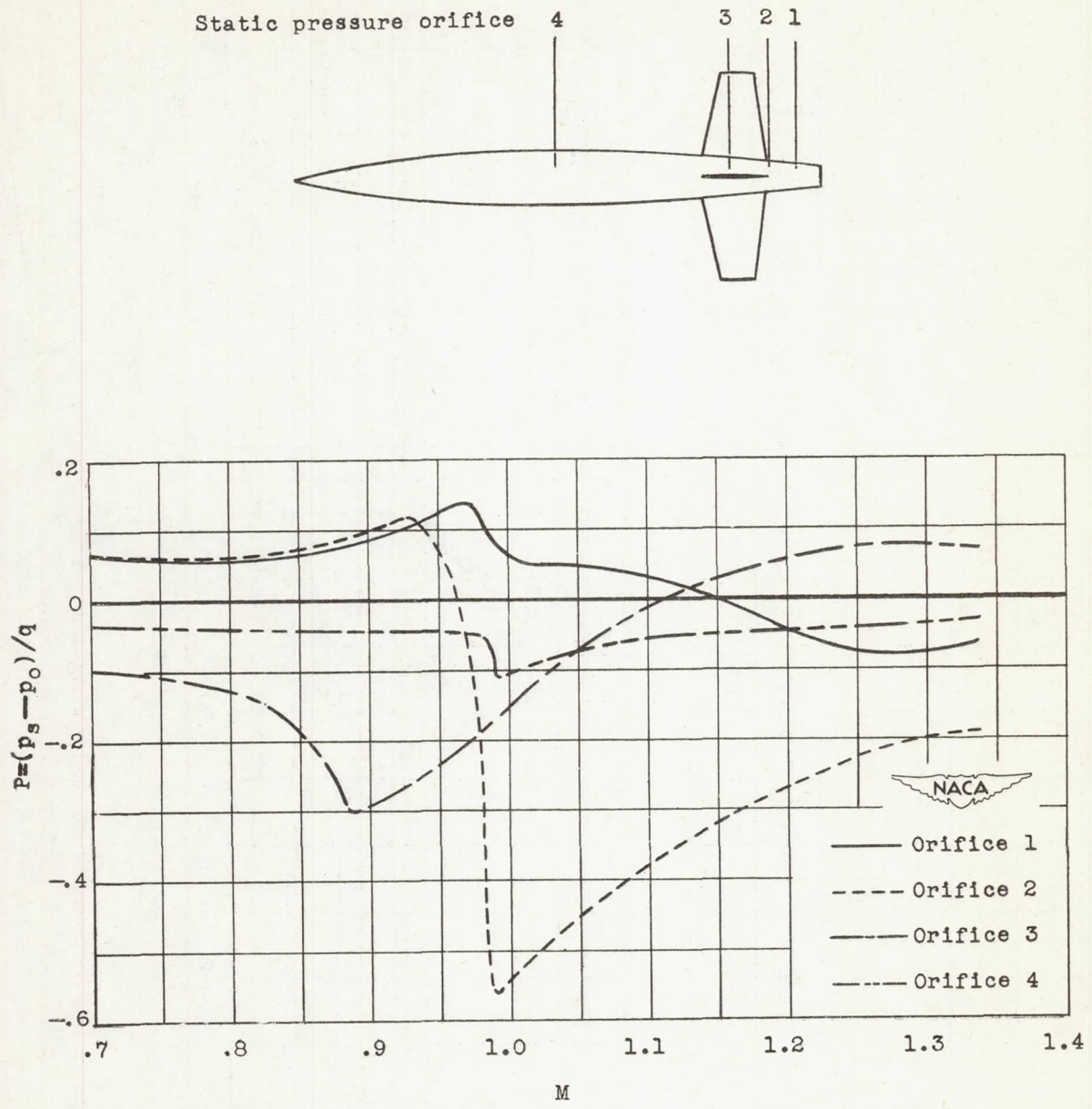

Figure 7.- Variation of side pressure coefficients with Mach number for model having 6-percent-thick wings. (Body pressures were measured on a plane midway between wings.)

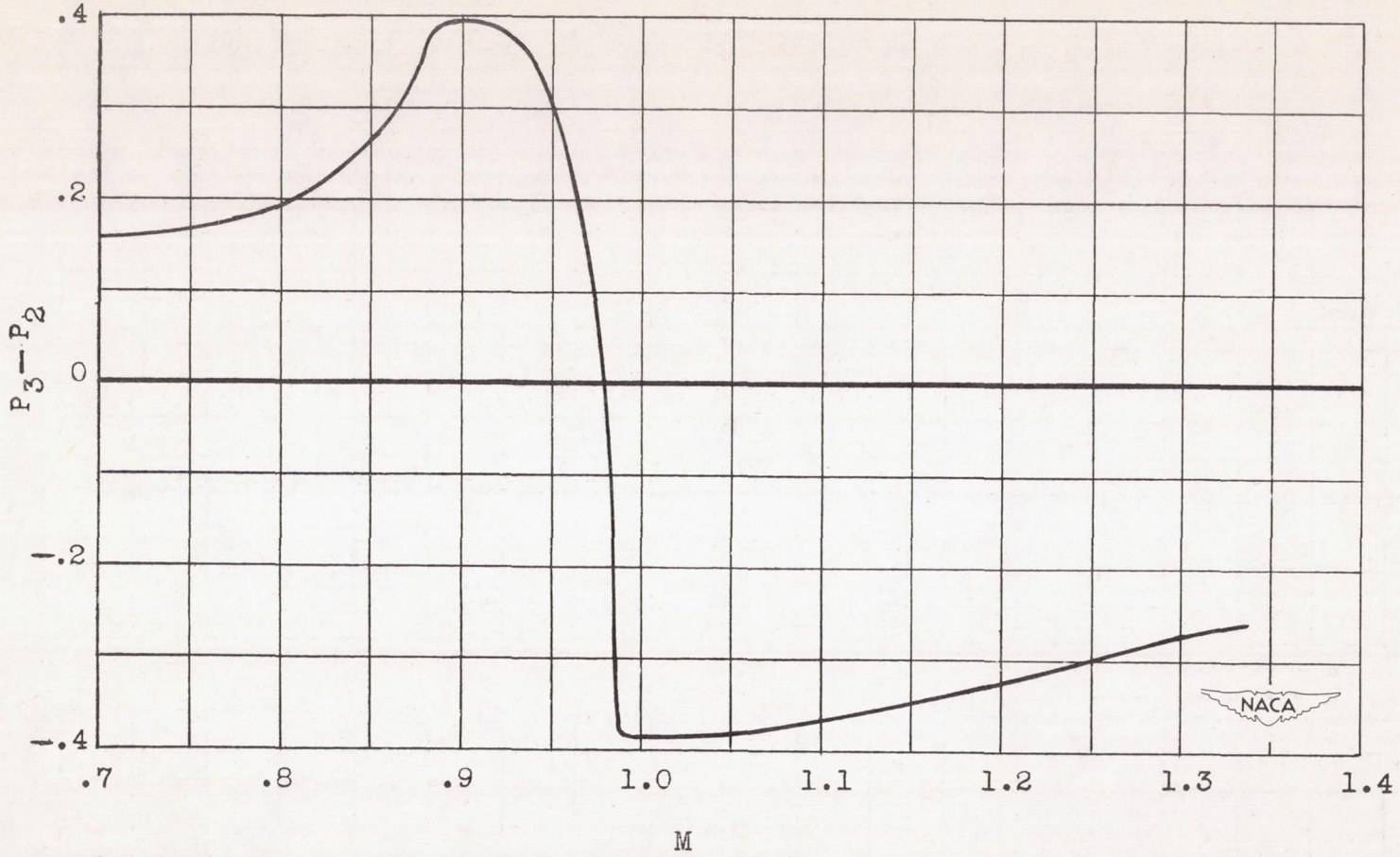

Figure 8.- Variation of side pressure gradient with Mach number between orifice 3 and orifice 2 on model having 6-percent-thick wings.

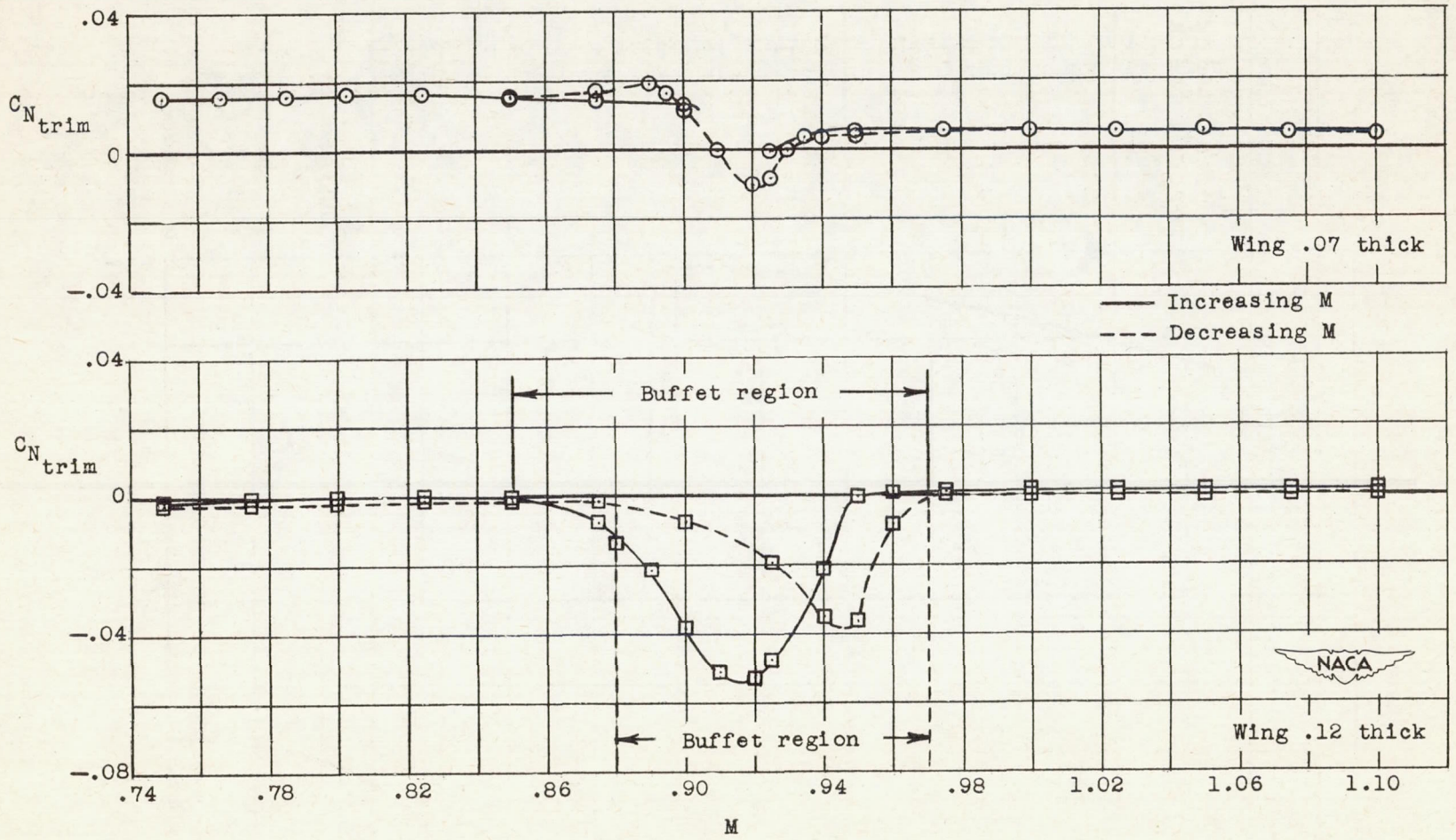

Figure 9.- Variation of trim normal-force coefficient with Mach number.

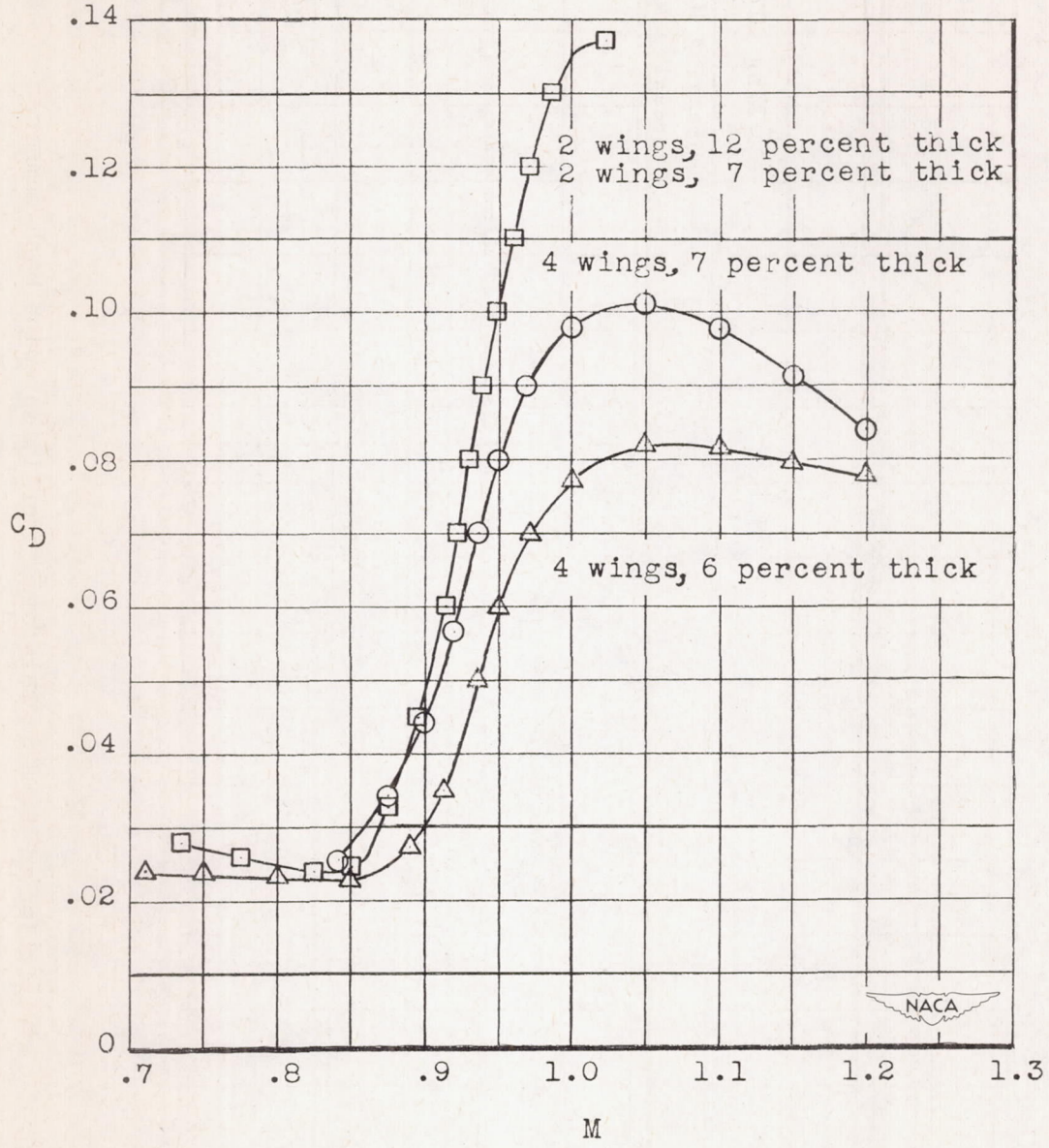

Figure 10.- Variation of total drag coefficient with Mach number. All drag coefficients are based on total area in one plane.